Available online at www.sciencedirect.com

SCIENCE DIRECT®

ELSEVIER

Polymer 47 (2006) 3826–3837

polymer

www.elsevier.com/locate/polymer

Isothermal and non-isothermal crystallization behavior of poly(L-lactic acid): Effects of stereocomplex as nucleating agent

Hideto Tsuji *, Hiroki Takai, Swapan Kumar Saha

Department of Ecological Engineering, Faculty of Engineering, Toyohashi University of Technology, Tempaku-cho, Toyohashi, Aichi 441-8580, Japan

Received 26 October 2005; received in revised form 15 February 2006; accepted 18 March 2006

Abstract

The effects of incorporated poly(D-lactic acid) (PDLA) as poly(lactic acid) (PLA) stereocomplex crystallites on the isothermal and non-isothermal crystallization behavior of poly(L-lactic acid) (PLLA) from the melt were investigated for a wide PDLA contents from 0.1 to 10 wt%. In isothermal crystallization from the melt, the radius growth rate of PLLA spherulites (crystallization temperature (T_c) ≥ 125 °C), the induction period for PLLA spherulite formation (t_i) ($T_c \geq 125$ °C), the growth mechanism of PLLA crystallites (90 °C ≤ T_c ≤ 150 °C), and the mechanical properties of the PLLA films were not affected by the incorporation of PDLA or the presence of stereocomplex crystallites as a nucleating agent. In contrast, the presence of stereocomplex crystallites significantly increased the number of PLLA spherulites per unit area or volume. In isothermal crystallization from the melt, at PDLA content of 10 wt%, the starting, half, and ending times for overall PLLA crystallization (t_c(S), t_c(1/2), and t_c(E), respectively) were much shorter than those at PDLA content of 0 wt%, due to the increased number of PLLA spherulites. Reversely, at PDLA content of 0.1 wt%, the t_c(S), t_c(1/2), and t_c(E) were longer than or similar to those at PDLA content of 0 wt%, probably due to the long t_i and the decreased number of spherulites. This seems to have been caused by free PDLA chains, which did not form stereocomplex crystallites. On the other hand, at PDLA contents of 0.3–3 wt%, the t_c(S), t_c(1/2), and t_c(E) were shorter than or similar to those at PDLA content of 0 wt% for the T_c range below 95 °C and above 125 °C, whereas this inclination was reversed for the T_c range of 100–120 °C. In the non-isothermal crystallization of as-cast or amorphous-made PLLA films during cooling from the melt, the addition of PDLA above 1 wt% was effective to accelerate overall PLLA crystallization. The X-ray diffractometry could trace the formation of stereocomplex crystallites in the melt-quenched PLLA films at PDLA contents above 1 wt%. This study revealed that the addition of small amounts of PDLA is effective to accelerate overall PLLA crystallization when the PDLA content and crystallization conditions are scrupulously selected.

Keywords: Stereocomplex; Poly(L-lactide); Nucleating agent

1. Introduction

Enhancement of heat-resistance or thermal stability of poly(L-lactic acid) (PLLA) is a matter of concern when PLLA is utilized for various applications including industrial applications [1–12]. Numerous studies have been carried out for improving the thermal stability of PLLA. Stereocomplexation between PLLA and poly(D-lactic acid) (PDLA) is one of the most effective and promising methods for increasing the thermal stability of poly(lactic acid) (PLA)-based materials [13–16]. Recently, we found that the overall crystallization rate of PLA stereocomplex is much higher than that of pure PLLA or PDLA, due to extremely high radius growth rate and density (number per unit area or volume) of stereocomplex spherulites and a very short induction period for the formation of stereocomplex spherulites compared to those of PLLA or PDLA spherulites [17]. However, a high production cost of PDLA is the bottleneck of the stereocomplexed PLA materials.

On the other hand, increasing the crystallinity by the addition of nucleators to PLLA is effective for the production of low-cost PLA-based materials with high thermal stability. Brochu et al. found that PLLA crystallization or growth of PLLA crystallites [melting temperature (T_m) = 170–180 °C] takes place epitaxially on the PLA stereocomplex crystallites (T_m = 220–230 °C) when the content of PDLA was as low as 10 wt% [18]. In other words, the stereocomplex crystallites can act as nucleation sites for PLLA. Schmidt and Hillmyer [19] and Yamane

---

* Corresponding author.
E-mail address: tsuji@eco.tut.ac.jp (H. Tsuji).

0032-3861/$ - see front matter © 2006 Elsevier Ltd. All rights reserved.
doi:10.1016/j.polymer.2006.03.074

and Sasai [20] confirmed that the addition of PDLA or the presence of stereocomplex crystallites is effective to increase the number of PLLA spherulites, and therefore, the overall crystallization rate. Schmidt and Hillmyer studied the concentration effects of added PDLA [number-average molecular weight (M_n) $= 1.5 \times 10^4$ g mol^{-1}, 0.25–15 wt%] on non-isothermal PLLA crystallization using multi-step process: the specimens were heated up to 240 °C and held for 5 min, quenched to 160 °C and then cooled slowly to 100 °C (formation of stereocomplex crystallites and PLLA crystallites), heated rapidly to 188 °C (partial melting: melting of PLLA crystallites and leaving the stereocomplex crystallites) and held for 5 min, and cooled slowly (crystallization behavior was observed here), and discussed the effectiveness of self nucleation by the partial melting. They indicated that addition of PDLA above 0.25 wt% is effective to enhance the overall PLLA crystallization in cooling after the aforementioned multiple process and in direct cooling from the melt, and that the crystallization temperature during cooling became higher with increasing the PDLA content. Yamane and Sasai investigated the effects of content (1–5 wt%) and molecular weight [weight-average molecular weight (M_w) $= 4.5 \times 10^4 - 2.6 \times 10^5$ g mol^{-1}] of PDLA on the isothermal and non-isothermal PLLA crystallization at a fixed temperature and during cooling from the melt, respectively. They revealed that high molecular weight PDLA is effective to enhance the overall PLLA crystallization even at a low PDLA content such as 1 wt%, and that the enhancement of overall PLLA crystallization was not observed when the stereocomplex crystallites in the films formed during solvent-casting were melted at 240 °C.

In our previous study [21], the isothermal crystallization of PLLA was investigated by three procedures, i.e. direct crystallization of as-cast specimens, crystallization from the melt of as-cast specimens, and direct crystallization of melt-quenched (amorphous-made) specimens. It was indicated that although melt-quenching before crystallization increases the number per unit area or volume of PLLA spherulites and elevates overall crystallization rate compared to those for direct crystallization from the melt, melt-quenching does not vary final crystalline thickness and crystallinity. The purpose of this study was to investigate in detail and comprehensively the effects of content of added PDLA and type of thermal procedures on the enhancement of overall crystallization of PLLA films containing different amounts of PDLA. For this purpose, the PLLA specimens containing 0.1–10 wt% of PDLA were prepared by solution-casting and two types of procedures were utilized for crystallization experiments; (1) crystallization at a fixed temperature directly from the melt (isothermal crystallization), (2) crystallization on cooling directly from the melt of as-cast or melt-quenched specimens (non-isothermal). The crystallization of PLLA was monitored by polarization optical microscopy, light transmittance measurements, and differential scanning calorimetry (DSC).

2. Experimental section

2.1. Materials

PLLA was kindly supplied by Unitika Co. (Kyoto, Japan), while PDLA was prepared by ring-opening polymerization of D-lactide in bulk at 140 °C initiated with stannous octoate (stannous 2-ethylhexanoate) (0.03 wt%) in the presence of lauryl alcohol as a coinitiator (0.5 wt%). Synthesized and supplied polymers were purified by precipitation using methylene chloride and methanol as solvent and non-solvent, respectively. The purified polymers were dried in vacuo for at least 7 days. The molecular characteristics of the polymers after purification are listed in Table 1. The films of 10 and 100 μm thickness used for crystallization experiments and physical measurements, respectively, were prepared by the following procedure. The solutions of PLLA and PDLA (0.3 g dL^{-1}) were separately prepared using methylene chloride as a solvent, the prepared solutions were mixed together with vigorous stirring, the solutions were cast onto petri dishes placed horizontally, and then the solvent was allowed to evaporate at 25 °C for approximately 1 day. Here, the polymer weights required for preparing the fixed thickness were calculated using a density of 1.3 g cm^{-3} [11]. The obtained films were dried in vacuo for at least 7 days. The melt-quenched films were prepared by the following procedure. Each of the as-cast films were sealed under a reduced pressure, melted at 200 °C for 3 min, and then quenched at 0 °C. In this study, codes PLLA-0, PLLA-0.1, PLLA-0.3, PLLA-1, PLLA-3, and PLLA-10 stand for the PLLA films containing 0, 0.1, 0.3, 1, 3, and 10 wt% of PDLA, respectively.

2.2. Crystallization

The crystallization of PLLA films containing different contents of PDLA was carried out two different procedures. For isothermal crystallization, the as-cast films were heated to 200 °C at a rate of 100 °C min^{-1} and held at the same temperature for 3 min, rapidly cooled to a desired crystallization temperature (T_c) at a rate of -100 °C min^{-1}, and then crystallized at T_c (crystallization was observed here, process A). For non-isothermal crystallization, the as-cast and melt-quenched films were heated to 200 °C at a rate of 10 °C min^{-1} and held at the same temperature for 3 min, then cooled at a rate of -1 °C min^{-1} (crystallization was observed here, process B). Here, a holding temperature of 200 °C was selected to melt the PLLA crystallites but not to melt the stereocomplex

Table 1
Molecular characteristics PLLA and PDLA

Code	$[\alpha]^{25}_{589}$ [a] (° dm^{-1} g^{-1} cm^3)	M_n (g mol^{-1})	M_w/M_n
PLLA	−154	1.2×10^5	1.8
PDLA	155	5.2×10^4	1.5

[a] Specific optical rotation ($[\alpha]^{25}_{589}$) was measured in chloroform at 1 g dL^{-1}, 25 °C, and a wave length of 589 nm.

crystallites. For isothermal crystallization in process A polarization optical microscopy, light transmittance measurements, and DSC were utilized to trace PLLA crystallization, while non-isothermal crystallization in process B solely DSC was used to monitor PLLA crystallization.

2.3. Measurements and observation

The weight- and number-average molecular weights (M_w and M_n, respectively) of polymers were evaluated in chloroform at 40 °C using a Tosoh (Tokyo, Japan) GPC system with two TSK gel columns (GMH_{XL}) using polystyrene standards. The specific optical rotation of polymers ($[\alpha]^{25}_{589}$) was measured in chloroform at a concentration of 1 g dL^{-1} and 25 °C using a JASCO (Tokyo, Japan) DIP-140 polarimeter at a wave length of 589 nm.

The over all crystallization behavior of PLLA was monitored by a Shimadzu (Kyoto, Japan) DSC-50 differential scanning calorimeter. The specimens (sample weight ca. 3 mg) were heated or cooled according to the aforementioned requirements under a nitrogen gas flow of 50 mL min^{-1}. The cold crystallization and melting temperatures (T_{cc} and T_m, respectively) and the enthalpy of cold crystallization and melting (ΔH_{cc} and ΔH_m, respectively) were calibrated using benzophenone, indium, and tin as standards. In the present study, we use T_{cc} and ΔH_{cc} only for process B. The spherulite growth in the films was observed using an Olympus (Tokyo, Japan) polarization

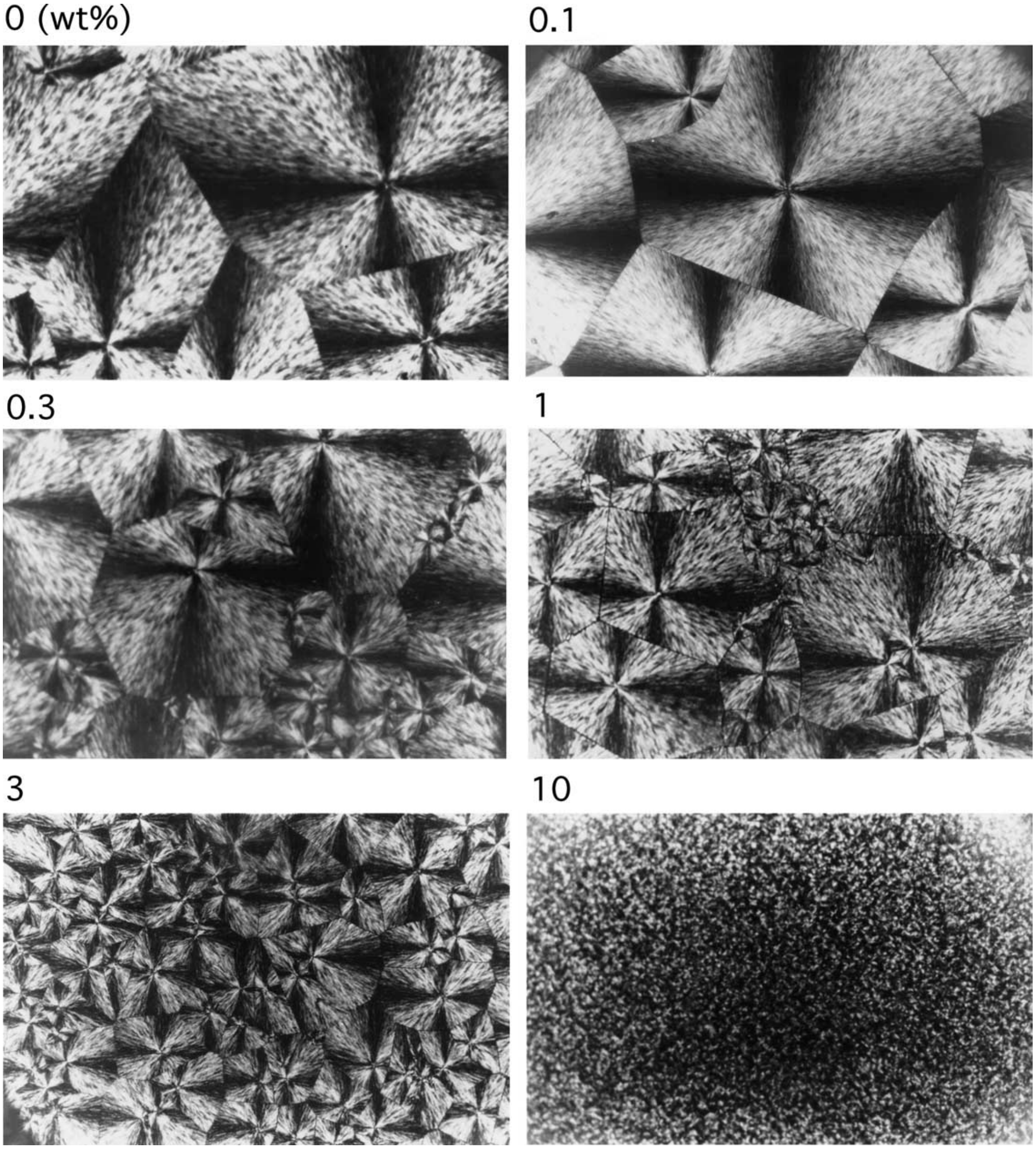

Fig. 1. Polarized optical photomicrographs of PLLA films containing different contents of PDLA crystallized at 135 °C after saturation of spherulite formation (Process A).

optical microscope (BX50) equipped with a heating-cooling stage and a temperature controller (Linkam LK-600PM) under a constant nitrogen gas flow. Overall crystallization behavior of PLLA was also monitored by light intensity transmitted through the specimens using the polarization optical microscope (BX-50) equipped with an As One (Osaka, Japan) LM-332 photometer.

X-ray diffractometry was performed at 25 °C using a Rigaku (Tokyo, Japan) RINT-2500 equipped with a Cu Kα source. The tensile properties of films (3 mm × 30 mm × 100 μm) were measured at 25 °C and 50% relative humidity using a tensile tester (EZ Test, Shimadzu Co.) at a cross-head speed of 100% min^{-1} (20 mm min^{-1}). The initial length between the two gauges was always kept at 20 mm.

3. Results and discussion

3.1. Isothermal crystallization

3.1.1. Spherulite growth behavior

First of all, we have investigated the spherulite growth behavior with process A by the use of polarization optical microscopy. Fig. 1 shows the polarized optical photomicrographs of PLLA films having different contents of PDLA taken at 135 °C after the saturation of spherulite formation. In Fig. 2, the PLLA spherulite density (number per unit area) estimated from the polarized optical photomicrographs is plotted as a function of T_c. As an approximate inclination, the number per unit area of PLLA spherulites increased with PDLA content, reflecting the fact that the stereocomplex crystallites formed in the films by the addition of PDLA acted effectively as a nucleating agent for PLLA spherulites or crystallites. Fig. 3 shows the radius growth rate (G) of PLLA spherulites and the induction period for PLLA spherulite formation (t_i) as a function of T_c. Here, G was estimated from the slope of spherulite radii plotted as a function of crystallization time (t_c), while t_i was evaluated from extrapolation of the spherulite radius lines plotted as a function of t_c to a radius of 0 μm [17,22,23]. The estimation of G and t_i was carried out for T_c above 125 °C, because too high density of PLLA spherulites at T_c

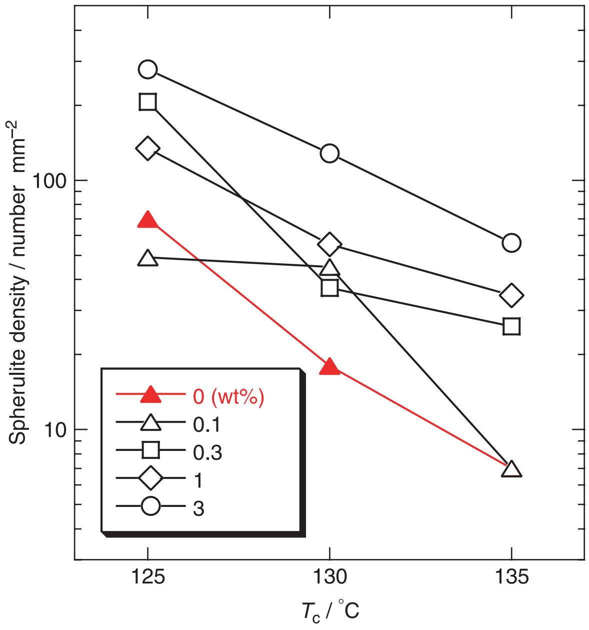

Fig. 2. Spherulite density (number per unit area) of PLLA films with different contents of PDLA as a function of T_c (process A).

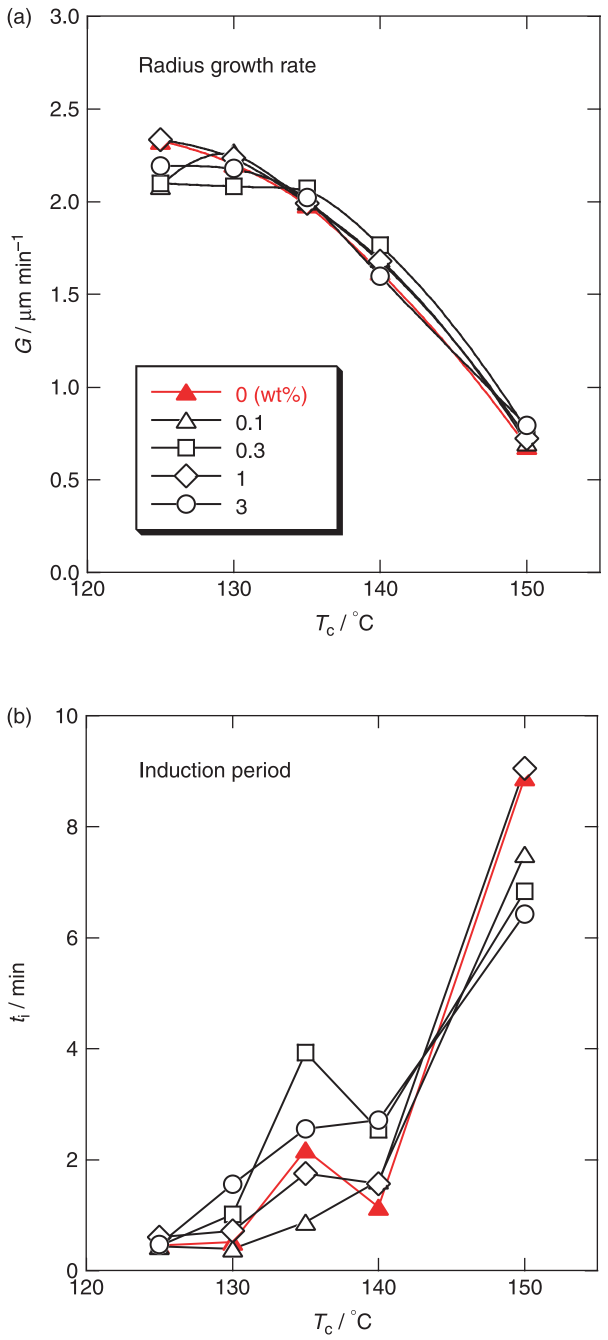

Fig. 3. Radius growth rate of PLLA spherulites (G) (a) and induction period for PLLA spherulite formation (t_i) (b) are plotted as a function of T_c (process A).

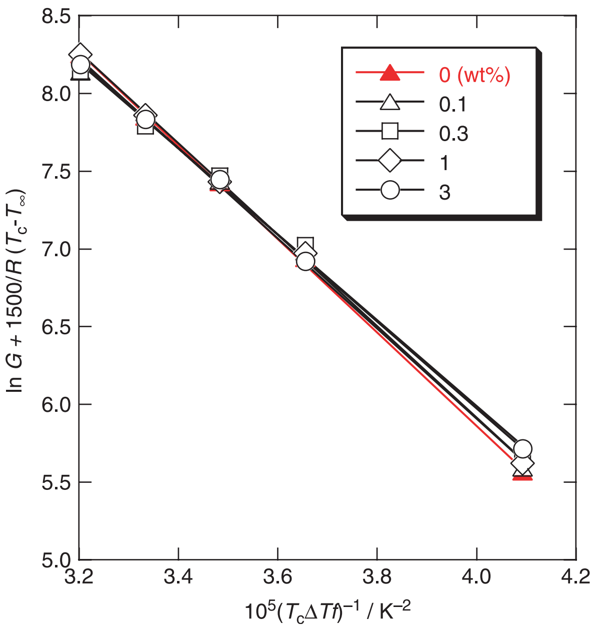

Fig. 4. ln $G+1500/R(T_c-T_\infty)$ of the films as a function of $1/(T_c\Delta Tf)$ (process A).

lower than 125 °C disturbed the estimation. Evidently, the G was approximately constant irrespective of PDLA content when compared at the same T_c. This reveals that the spherulites contained solely PLLA crystallites but not the stereocomplex crystallites, except for those as nucleation sites locating at the centers of PLLA spherulties. If a significant amount of stereocomplex crystallites were contained in the spherulites other than their centers, enormously high G values observed for sterteocomplex spherulites should have increased the observed G values in the present study [17]. On the other hand, although t_i increased with T_c, which is general inclination for PLLA spherulite formation [17,22,23], the t_i showed no explicit dependence on PDLA content. This means that the presence of stereocomplex crystallites does not affect the t_i.

We have estimated the nucleation constant (K_g) and the front constant (G_0) for the films by the use of nucleation theory established by Hoffman et al. [24,25], in which G can be expressed by the following equation

$$G = G_0\exp\left[\frac{-U^*}{R(T_c-T_\infty)}\right]\exp\left[\frac{-K_g}{(T_c\Delta Tf)}\right] \qquad (1)$$

where ΔT is undercooling $T_m^0-T_c$ where T_m^0 is equilibrium T_m, f is the factor expressed by $2T_c/(T_m^0+T_c)$ that accounts for the change in heat of function as the T_c is decreased below T_m^0, U^* is the activation energy for transportation of segments to the crystallization site, R is the gas constant, and T_∞ is the hypothetical temperature where all motion associated with viscous flow ceases. Fig. 4 shows the $\ln G+1500/R(T_c-T_\infty)$ of the films as a function of $1/(T_c\Delta Tf)$ under the assumption that T_m^0 is 212 °C [21]. Here, we used the universal values of $U^*=1500\ \mathrm{cal\ mol^{-1}}$ and $T_\infty=T_g-30\ \mathrm{K}$ for comparison between the reported values and ours [22,23,26–30]. The plot in Fig. 4 gives K_g as a slope and the intercept $\ln G_0$. Thus obtained K_g and G_0 values are summarized in Table 2. The transition temperature from regime II kinetics to regime III kinetics [$T_{c(\mathrm{II–III})}$] was ca. 120 °C [22,23,26,27,31,32] for PLLA having M_n above $3.1\times10^4\ \mathrm{g\ mol^{-1}}$. Therefore, in the T_c range studied here (125–150 °C), PLLA should have crystallized according to Regime II kinetics. The K_g values for regime II [K_g(II)] 2.76–3.01×$10^5\ \mathrm{K^2}$ obtained in the present study are in agreement with reported K_g(II) values, 2.29–2.44×$10^5\ \mathrm{K^2}$ ($M_v=1.5\times10^5$–$6.9\times10^5\ \mathrm{g\ mol^{-1}}$, Vasanthakumari and Pennings) [26], $1.92\times10^5\ \mathrm{K^2}$ ($M_n=6.6\times10^4\ \mathrm{g\ mol^{-1}}$, Baratian et al.) [30], $2.4\times10^5\ \mathrm{K^2}$ ($M_n=6.6\times10^4\ \mathrm{g\ mol^{-1}}$, Huang et al.) [29], $1.85\times10^5\ \mathrm{K^2}$ ($M_w=1.0\times10^5\ \mathrm{g\ mol^{-1}}$, Di Lorenzo) [31], 2.27–2.52×$10^5\ \mathrm{K^2}$ ($M_n=3.1\times10^4$–$5.6\times10^5\ \mathrm{g\ mol^{-1}}$, Tsuji et al.) [22,23]. The G_0 values for regime II [G_0(II)] of the films are 2.42–5.94×$10^7\ \mathrm{\mu m\ min^{-1}}$, also in agreement with 1.56–3.38×$10^7\ \mathrm{\mu m\ min^{-1}}$ reported by Vasanthakumari and Pennings [26] and 1.79–3.98×$10^7\ \mathrm{\mu m\ min^{-1}}$ reported by Tsuji et al. [22,23]. The K_g(II) and G_0(II) values did not have explicit dependence on the PDLA content, reflecting the fact that the addition of PDLA or the presence of PLA stereocomplex did not vary the growth mechanism of PLLA crystallites.

3.1.2. Overall crystallization behavior

To investigate overall crystallization behavior, we estimated the time change of the light intensity transmitted

Table 2

Estimated front constants [G_0 and $t_c(1/2)$] and nucleation constant (K_g) estimated from G and $t_c(1/2)$ values using Eqs. (1) and (5), respectively (process A)

	Estimated from G values		Estimated from $t_{1/2}$ values				
PDLA content (wt%)	G_0(II) [a] (μm min^{-1})	K_g (II)[a] (K^2)	$T_{c(\mathrm{II–III})}$ [a] (°C)	[$1/t_c(1/2)$]$_0$ (II) [a] (min^{-1})	[$1/t_c(1/2)$]$_0$ (III) [a] (min^{-1})	K_g (II)[a](K^2)	K_g(III) [a] (K^2)
0	5.94×10^7	3.01×10^5	110	3.27×10^6	7.16×10^{12}	3.95×10^5	9.00×10^5
0.1	3.98×10^7	2.90×10^5	110	5.39×10^6	2.63×10^{13}	4.15×10^5	9.48×10^5
0.3	2.42×10^7	2.76×10^5	110	1.98×10^7	7.98×10^9	4.60×10^5	6.60×10^5
1	4.86×10^7	2.94×10^5	110	2.19×10^7	1.45×10^{10}	4.60×10^5	6.87×10^5
3	2.67×10^7	2.79×10^5	110	1.09×10^7	1.60×10^{12}	4.37×10^5	8.53×10^5
10	–[b]	–[b]	110	4.88×10^6	1.18×10^{12}	4.04×10^5	8.38×10^5

[a] (II) and (III) mean regimes II and III, respectively.

[b] Spherulite density (number per unit area) was too high to estimate G values.

through the specimens (I) in polarization optical microscopy. The transmitted light intensity increases with the increase in crystallinity and finally levels off when crystallization completes. We used the relative light intensity (I_r) defined by the following equation as an index of crystallinity

$$I_r(\%) = 100 \times \frac{(I_t - I_0)}{(I_\infty - I_0)} \qquad (2)$$

where I_t and I_0 are the I values at $t_c = t$ and 0, respectively, I_∞ is the I value when it leveled off. Fig. 5 shows the typical I_t change with t_c for PLLA-0.1 film, where the starting, half, and ending times for overall PLLA crystallization [t_c(S), t_c(1/2), and t_c(E), respectively] are defined. The t_c(S) and t_c(E) were estimated from extrapolation of a contacting line of I_r to 0 and 100%, respectively. The evaluated t_c(S), t_c(1/2), and t_c(E) are plotted in Fig. 6 as a function of T_c. As shown in Fig. 6, the t_c(S) of the PLLA films with 0.1–3% of PDLA was longer than or similar to that of pure PLLA film (PLLA-0 film), whereas the t_c(S) of the PLLA film with 10 wt% of PDLA (PLLA-10 film) was shorter than that of PLLA-0 film. The PLLA-0.1 and PLLA-10 films, respectively, had the longest and shortest t_c(S), t_c(1/2), and t_c(E) among the films. The short t_c(1/2) and t_c(E) as observed for PLLA-10 film must be ascribed to the increased number of PLLA spherulites formed in the presence of sterecomplex crystallites, as shown in Fig. 2. In contrast, the long t_c(S), t_c(1/2) and t_c(E) as observed for PLLA-0.1 films can be attributed to the long t_i and the decreased number of spherulites. This seems to have been caused by free PDLA chains, which did not form stereocomplex crystallites. At T_c below 95 °C and above 125 °C, t_c(1/2) and t_c(E) were shorter for the PLLA films containing 0.3–3 wt% of PDLA than for PLLA-0 film, whereas this inclination was reversed at T_c of 100–115 °C.

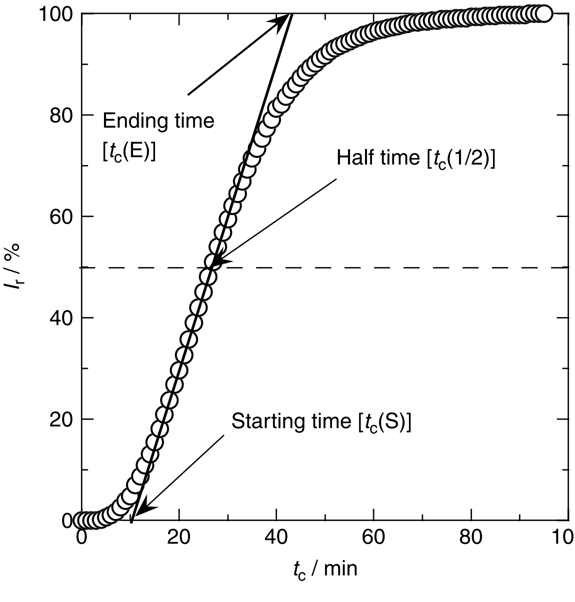

Fig. 5. Typical I_r change with crystallization time (t_c) obtained for PLLA-0.1 film at 125 °C (process A).

Isothermal crystallization kinetics traced by light intensity were analyzed with the Avrami theory [33–35], which is expressed in the following equation

$$1 - \frac{x_t}{100} = \exp(-k t_c^n) \qquad (3)$$

where x_t is percentage of relative crystallization, k is the crystallization rate constant. Equation (3) can be transformed to equation (4).

$$\ln\left[-\ln\left(1 - \frac{x_t}{100}\right)\right] = \ln k + n \ln t_c \qquad (4)$$

In this study, we used I_r as x_t in equation (4). To avoid the deviation from the theoretical curves, as stated by Mandelkern [36] at I_r exceeding 25%, we used I_r lower than 25% for estimating n and $\ln k$. A typical plot is given for PLLA-0 film in Fig. 7, and such plots give n as a slope and the intercept $\ln k$. Obtained n and $\ln k$ values are listed in Table 3. The estimated n values were ca. 3 for the films, except for those at $T_c = 90$ °C, irrespective of the content of PDLA. This is an indication that the growing of crystallites is three-dimensional and athermal [32]. The obtained n values were similar to those reported for pure PLLA (2.5–3.3 at $T_c = 90$–130 °C by Kolstad [37] and 2.8–3.2 at $T_c =$ 90–130 °C by Iannace and Nicolais [38]), but slightly smaller than ca. 4 at $T_c = 110$–132.5 °C reported by Miyata and Masuko [28]. The value difference is attributable to the differences in the method for monitoring crystallinity, in the T_c range for the crystallization experiments, and in the relative crystallinity range used for the calculation.

Using the theoretical approach that G is considered to be proportional to $1/t_c(1/2)$ and based on the Hoffman–Lauritzen theory [39–41] the temperature variation of $1/t_c(1/2)$ is written as:

$$\left[\frac{1}{t_c(1/2)}\right] = \left[\frac{1}{t_c(1/2)}\right]_0 \exp\left[-\frac{U^*}{R(T_c - T_\infty)}\right] \exp\left[-\frac{K_g}{T_c \Delta T f}\right] \qquad (5)$$

Fig. 8 shows the $\ln[1/t_c(1/2)] + 1500/R(T_c - T_\infty)$ of the films as a function of $1/(T_c \Delta T f)$ under the assumption that T_m^0 is 212 °C [21]. Again, we used the universal values of $U^* = 1500\ \mathrm{cal\ mol^{-1}}$ and $T_\infty = T_g$–30 K for comparison between the reported values and ours [22,23,26–30]. Fig. 8 gives K_g as a slope and the intercept $\ln[1/t_c(1/2)]_0$. Some data in Fig. 8 are composed of two lines having different slopes. In these cases, we assumed the lines having high and low slopes were for regime III and regime II kinetics, respectively, and estimated K_g and $[1/t_c(1/2)]_0$ values for these two lines. This assumption is validated because in the case of pure PLLA the K_g values for regime III [K_g(III)] were twice those for regime II [K_g(II)] (Table 2). The transition temperature from regime II kinetics to regime III obtained here is constant (110 °C) and slightly lower than 120 °C reported in previous articles

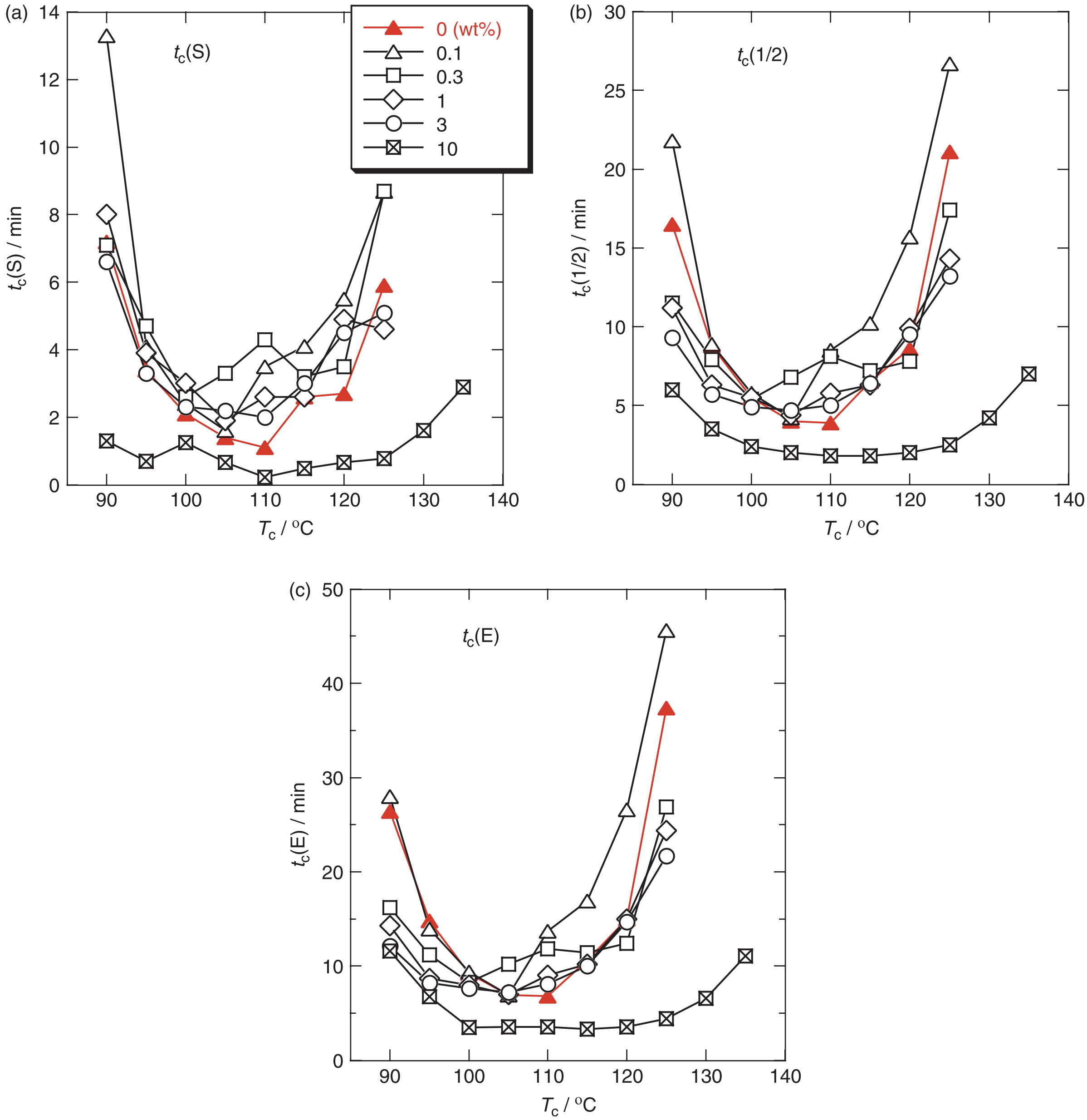

Fig. 6. Starting, half, and ending times for overall PLLA crystallization [t_c(S) (a), t_c(1/2) (b), and t_c(E) (c), respectively] of films with different contents of PDLA as a function of T_c (process A).

estimated using G values [22,23,26,27,31,32]. This indicates that incorporation of PDLA does not alter the temperature dependence on the growth mechanism of PLLA crystallites and that $T_{c(II–III)}$ can vary depending on the estimating method.

As shown in Table 2, for PLLA-0 film the K_g(II) value estimated using $1/t_c(1/2)$ (3.95×10^5 K^2) are slightly higher than that evaluated using G (3.01×10^5 K^2). Similar to K_g(II) values, the K_g(III) value estimated using $1/t_c(1/2)$ (9.00×10^5 K^2) (Table 2) is larger than those evaluated using G in the previous studies (4.38×10^5 K^2 [31], 4.60–5.51 K^2 [22,23]). However, both K_g and $[1/t_c(1/2)]_0$ values did not show explicit dependence on PDLA content, confirming the fact that the presence of stereocomplex crystallites as a nucleating agent does not affect the growth mechanism of the PLLA crystallites.

3.1.3. Physical properties after the completion of crystallization

The non-normalized and normalized ΔH_m and T_m values of the PLLA films with different contents of PDLA after crystallization at 135 °C for 10 h are given in Table 4. Here, ΔH_m was normalized by the fraction of crystallizable PLLA from non-normalized ΔH_m according to the following equation, which assumes that added PDLA chains and the same amount of PLLA chains form stereocomplex crystallites

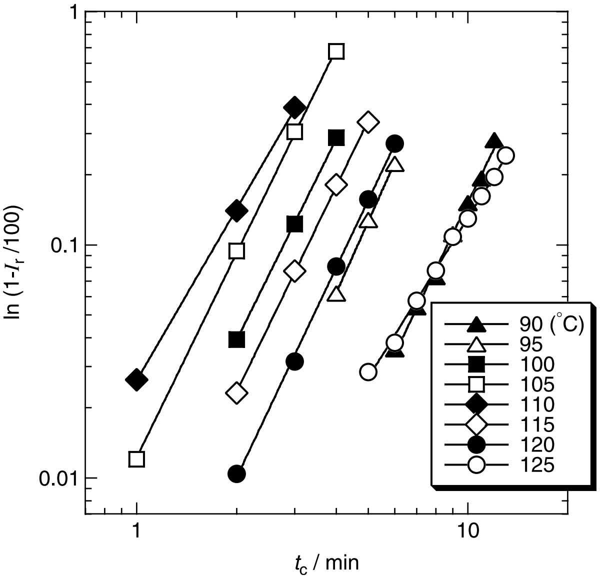

Fig. 7. $1-I_r/100$ of PLLA-0 film as a function of crystallization time (t_c) (process A).

Table 3
The Avrami exponent (n) and the crystallization rate constant (k) of PLLA films with different contents of PDLA (process A)

PDLA content (wt%)	T_c (°C)	n	$-\ln k$ (min^{-n})
0	90	2.94	8.65
	95	3.17	7.17
	100	2.87	5.24
	105	2.91	4.41
	110	2.44	5.94
	115	2.93	5.79
	120	2.99	6.68
	125	2.28	7.28
0.1	90	3.05	11.24
	95	3.01	7.00
	100	3.01	5.53
	105	2.85	4.40
	110	2.89	6.50
	115	3.30	7.89
	120	3.14	8.75
	125	2.93	9.72
0.3	90	7.18	17.24
	95	3.84	8.46
	100	2.91	5.32
	105	2.84	5.89
	110	2.86	6.42
	115	2.96	6.16
	120	3.23	6.95
	125	3.20	9.54
1	90	5.27	13.19
	95	4.49	8.68
	100	4.05	7.15
	105	2.80	4.53
	110	2.60	5.08
	115	2.88	5.74
	120	3.38	8.03
	125	2.87	7.77
3	90	4.66	11.02
	95	3.12	6.02
	100	2.86	5.01
	105	4.05	7.36
	110	2.72	4.72
	115	2.99	5.94
	120	3.05	7.24
	125	2.89	7.73
10	90	3.58	6.67
	95	3.05	4.25
	100	2.75	5.01
	105	4.01	7.36
	110	2.04	1.50
	115	2.50	1.81
	120	2.72	2.25
	125	2.86	2.98
	130	2.98	4.41
	135	3.44	6.79

and such PLLA chains were no more crystallizable:

$$\text{Normalized } \Delta H_m(\text{J g}^{-1}) = \text{Non-normalized } \Delta H_m(\text{J g}^{-1})/[1-2\times\text{PDLA content (wt\%)}/100] \quad (6)$$

The non-normalized and normalized ΔH_m and T_m decreased at PDLA content above 3 wt%. Although the presence of stereocomplex crystallites accelerates overall PLLA crystallization at the PDLA content of 10 wt%, the finial growth of PLLA crysatllites is significantly disturbed by the presence of stereocomplex crystallites, resulting in the decreased ΔH_m and T_m values. Despite the significant dependence of non-normalized and normalized ΔH_m and T_m on PDLA content, the tensile properties of the PLLA films were practically constant, irrespective of PDLA content. This revels that the presence of PDLA or stereocomplex crystallites as the nucleating agent does not affect the mechanical properties of PLLA films.

3.2. Non-isothermal crystallization

We have carried out further investigation to obtain the information useful for industrial applications of the stereocomplex crystallites as a nucleating agent. Fig. 9 shows DSC thermograms (cooling at a rate of −1 °C min^{-1} from the melt, process B) of as-cast and melt-quenched PLLA films containing different amounts of PDLA from the melt. Starting, peak, and ending temperatures [T_{cc}(S), T_{cc}(P), and T_{cc}(E), respectively] for PLLA crystallization and normalized and non-normalized $-\Delta H_{cc}$ of the as-cast and melt-quenched films during cooling from the melt were estimated from Fig. 9 and given in Fig. 10 and Table 5. The T_{cc}(S), T_{cc}(P), and T_{cc}(E) for PLLA crystallization in Fig. 10 were obtained as follows. The T_{cc}(P) is the peak top temperature of crystallization peak, while the T_{cc}(S) and T_{cc}(E) are the intersection temperatures of the base line and the tangent lines for the crystallization curves lower and higher than T_{cc}(P), respectively. In Table 5, $-\Delta H_{cc}$ was normalized by the fraction of crystallizable PLLA from non-normalized $-\Delta H_{cc}$ according to the following equation, which assumes that added PDLA chains and the same amount

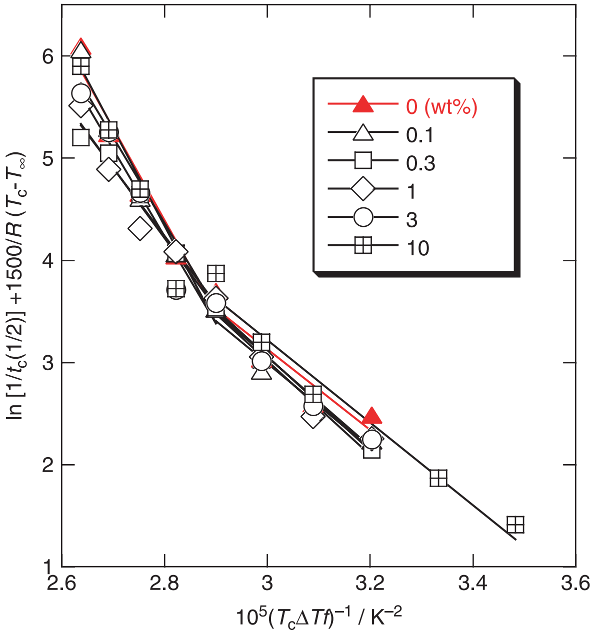

Fig. 8. $\ln[1/t_c(1/2)]+1500/R(T_c-T_\infty)$ of the films as a function of $1/(T_c\Delta Tf)$ (process A).

of PLLA chains form stereocomplex crystallites and these PLLA chains were no more crystallizable:

$$\text{Normalized } -\Delta H_{cc}(\mathrm{J\,g^{-1}}) = \text{Non}-\text{normalized } -\Delta H_{cc}(\mathrm{J\,g^{-1}})/[1-2\times \text{PDLA content (wt\%)}/100] \quad (7)$$

At the cooling rate of $-1\,°\mathrm{C\,min^{-1}}$, the peak crystallization temperatures of as-cast and melt-quenched PLLA-0 films, 113.2 and 121.7 °C are slightly higher and much higher than 106.0 °C reported by Migliaresi et al. for pure PLLA with viscosity-average molecular weight (M_v) of $4.25\times10^5\,\mathrm{g\,mol^{-1}}$ [42]. The $-\Delta H_{cc}$ values of as-cast and melt-quenched PLLA-0 films, 41.9 and $43.7\,\mathrm{J\,g^{-1}}$, are, respectively, higher than $34.0\,\mathrm{J\,g^{-1}}$ reported by Migliaresi et al. [42]. At the PDLA contents above 1 wt%, the T_{cc}(S), T_{cc}(P), and T_{cc}(E) were higher for the PLLA films containing PDLA than for PLLA-0 film, whereas this trend was reversed for the T_{cc}(P) and T_{cc}(E) at the PDLA contents of 0.1 and 0.3 wt%. This finding indicates that the addition of PDLA at the content above 1 wt% accelerates the overall PLLA crystallization, probably due to the increased spherulite density by the presence of stereocomplex crystallites, as revealed from the experiments of isothermal crystallization (Fig. 2). On the other hand, at PDLA contents of 0.1 and 0.3, it seems that the PDLA chains, which did not form stereocomplex crystallites, disturbed the formation and growth of PLLA spherulites. When compared at the same PDLA content, all the T_{cc} values were higher for the as-cast PLLA films than for the melt-quenched films. This means that repeated melting reduces the enhancement effects of the stereocomplex crystallites. On the other hand, the normalized $-\Delta H_{cc}$ values were almost constant, excluding the as-cast PLLA-0.1 film (Table 5). This indicates that the final crystallinity of PLLA in the films is not influenced by the presence of stereocomplex crystallites as a nucleating agent. In addition to this inclination, the non-normalized $-\Delta H_{cc}$ values decreased for PDLA content exceeding 1 wt% because at higher PDLA contents the stereocomplexed PLLA and PDLA cannot take part in formation of PLLA crystallites.

3.3. X-ray diffractometry

In order to investigate or confirm the formation of stereocomplex crystallites, we have carried out the X-ray diffractometry of the melt-quenched films with different contents of PDLA prepared by melting at 200 °C for 3 min and subsequent quenching at 0 °C (Fig. 11). The highly ordered structures of the melt-quenched films are identical to those at the initial stage before isothermal or non-isothermal crystallization. At PDLA contents of 3 and 10 wt%, the typical diffraction peaks (12, 21, and 24°) [43] of stereocomplex crystallites were observed, although at 3 wt% the diffraction peak at 24° was not clearly noticed probably because the peak intensity was comparable to the noise level. This confirms the formation of stererocomplex crystallites at these PDLA contents. At 1 wt%, only the diffraction peak at 12° was

Table 4
The final non-normalized and normalized ΔH_m, T_m, and mechanical properties of PLLA films with different contents of PDLA after crystallization at 135 °C for 10 h (process A)

PDLA content (wt%)	Non-normalized ΔH_m ($\mathrm{J\,g^{-1}}$)	Normalized ΔH_m ($\mathrm{J\,g^{-1}}$)	T_m (°C)	TS[a] (MPa)	YM[b] (GPa)	EB[c] (%)
0	55.4	55.4	171.3	50.7	1.29	6.3
0.1	58.9	59.0	170.8	41.6	0.99	5.1
0.3	54.9	55.2	171.1	53.4	0.96	7.6
1	54.9	56.0	171.2	45.3	1.18	6.1
3	46.8	49.8	170.1	54.1	1.32	7.3
10	39.9	49.9	169.7	53.6	1.10	8.7

[a] Tensile strength.
[b] Young's modulus.
[c] Elongation-at-break.

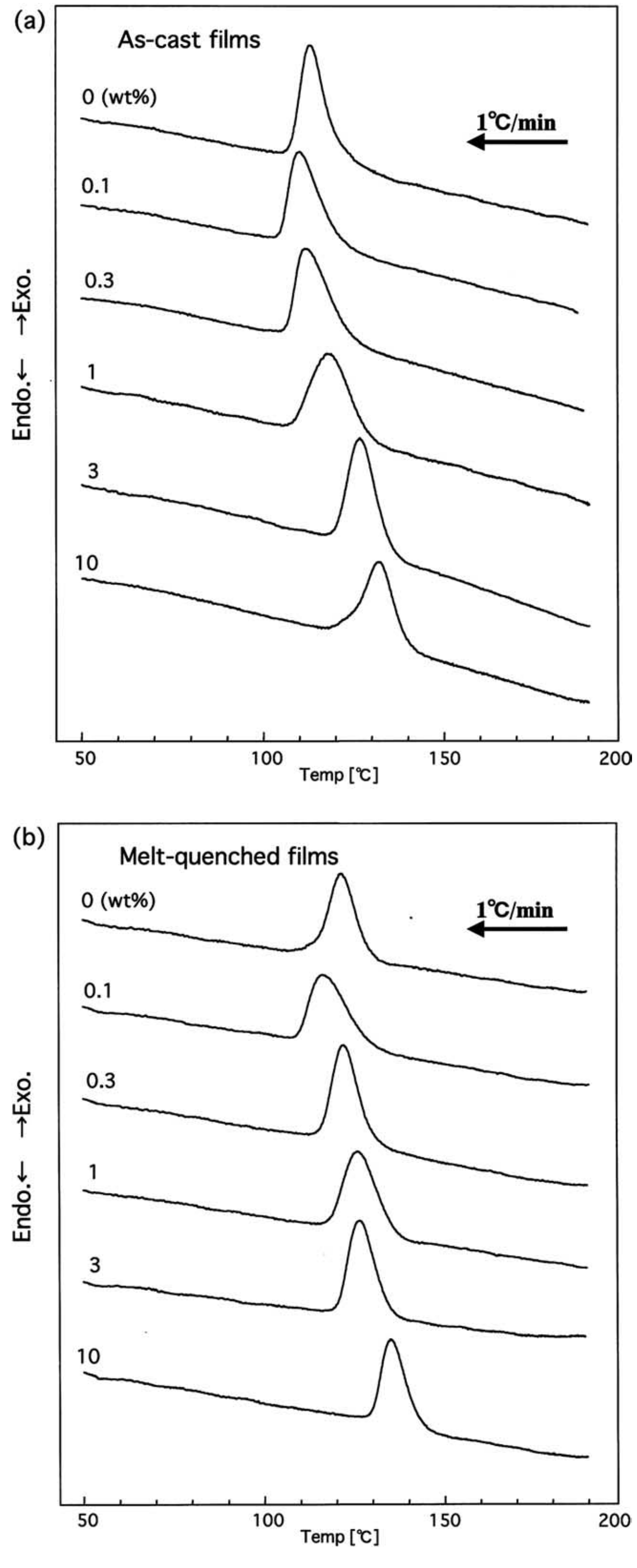

Fig. 9. DSC thermograms (cooling) of as-cast (a) and melt-quenched (b) PLLA films with different contents of PDLA from the melt (process B).

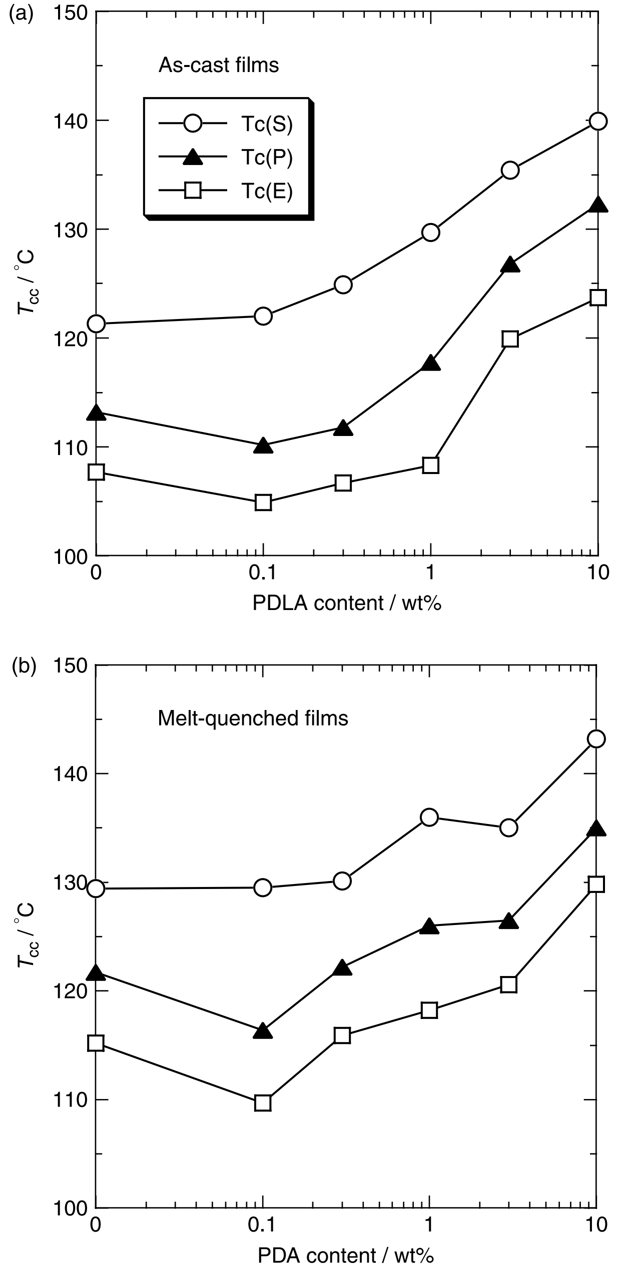

Fig. 10. Starting, peak, and ending temperatures [T_{cc}(S), T_{cc}(P), and T_{cc}(E), respectively] for PLLA crystallization of as-cast (a) and melt-quenched (b) films during cooling from the melt as a function of PDLA content (process B).

observed. However, this also means the formation of stereocomplex crystallites. As far as we are aware, this is the first report that confirmed the formation of stereocomplex crystallites at the PDLA content as low as 1 wt%. At PDLA contents lower than 1 wt%, no sharp diffraction peak attributed to crystalline structure could be noticed. This reflects that the specimens were completely amorphous or the amounts of stereocomplex crystallites were too low to be traced by X-ray diffractometry. The formation of sterteocomplex crystallites at the PDLA contents above 1 wt% coincides well with the fact that the enhancement of overall isothermal and non-isothermal crystallization of PLLA at relatively high PDLA contents.

4. Conclusions

From the aforementioned experimental results the following conclusions can be derived for the effects of addition of PDLA

Table 5
The T_{cc} and $-\Delta H_{cc}$ of as-cast films and melt-quenched films during cooling from the melt (process B)

PDLA content (wt%)	T_{cc}(S) (°C)	T_{cc}(P) (°C)	T_{cc}(E) (°C)	Non-normalized $-\Delta H_{cc}$ (J g^{-1})	Normalized $-\Delta H_{cc}$ (J g^{-1})
(a) As-cast films					
0	121.3	113.2	107.7	41.9	41.9
0.1	122.0	110.2	104.9	36.2	36.3
0.3	124.9	111.8	106.7	40.3	40.5
1	129.7	117.8	108.3	40.8	41.6
3	135.4	126.8	119.9	38.9	41.4
10	139.9	132.3	123.7	33.5	41.9
(b) Melt-quenched files					
0	129.4	121.7	115.2	43.7	43.7
0.1	129.5	116.4	109.7	42.2	42.3
0.3	130.1	122.2	115.9	40.8	41.0
1	136.0	126.0	118.2	41.7	42.6
3	135.0	126.5	120.6	37.3	39.7
10	143.2	135.0	129.8	30.5	38.1

on isothermal and non-isothermal crystallization behavior of PLLA from the melt:

(1) In isothermal crystallization from the melt, the G ($T_c \geq 125$ °C), the t_i ($T_c \geq 125$ °C), the growth mechanism of PLLA crystallites (90 °C $\leq T_c \leq$ 150 °C), and the mechanical properties of the PLLA films were not affected by the presence of stereocomplex crystallites as a nucleating agent. In contrast, the presence of stereocomplex crystallites significantly increased the number of PLLA spherulites per unit area or volume.

(2) In isothermal crystallization from the melt, at PDLA content of 10 wt%, the t_c(S), t_c(1/2), and t_c(E) were much shorter than those at PDLA content of 0 wt%, due to the increased number of PLLA spherulites. Reversely, at PDLA content of 0.1 wt%, the t_c(S), t_c(1/2), and t_c(E) were longer than or similar to those at PDLA content of 0 wt%, probably due to the long t_i and the decreased number of spherulites. This seems to have been caused by free PDLA chains, which did not form stereocomplex crystallites. On the other hand, at PDLA contents of 0.3–3 wt%, the t_c(S), t_c(1/2), and t_c(E) were shorter than or similar to those at PDLA content of 0 wt% for the T_c range below 95 °C and above 125 °C, whereas this inclination was reversed for the T_c range of 100–120 °C.

(3) In the case of non-isothermal crystallization during cooling from the melt, the addition of PDLA above 1 wt% was effective to accelerate overall PLLA crystallization. The enhancement was more dramatic for the as-cast films than for melt-quenched films.

(4) X-ray diffractometry could trace the formation of stereocomplex crystallites in the melt-quenched PLLA films at PDLA contents above 1 wt%.

(5) This study revealed that the addition of small amounts of PDLA is effective to accelerate overall PLLA crystallization when the PDLA content and crystallization conditions are scrupulously selected.

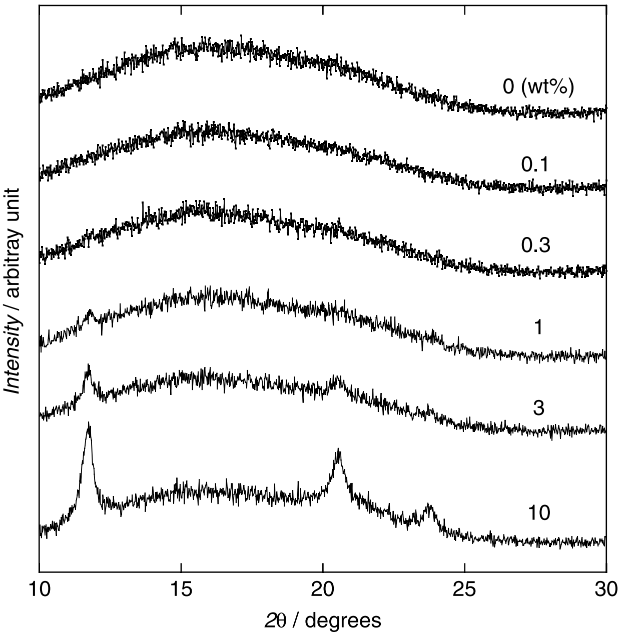

Fig. 11. X-ray diffraction profiles of melt-quenched PLLA films with different contents of PDLA at 25 °C.

Acknowledgements

We are grateful to Professor Dr Shinichi Itsuno, from Department of Materials Science, Toyohashi University of Technology for the use of the polarimeter facility and to Mr Kazunobu Yamada, from Research and Development Center, Unitika Ltd, for giving us PLLA used in the present study. This research was supported by a Grant-in-Aid for Scientific Research on Priority Area, 'Sustainable Biodegradable Plastics' No.11217209, and The 21st Century COE Program, 'Ecological Engineering for Homeostatic Human Activities', from the Ministry of Education, Culture, Sports, Science and Technology (Japan), and a Grand-in-aid for Scientific Research, Category 'C', No. 16500291, from Japan Society for the Promotion of Science (JSPS).

References

[1] Kharas GB, Sanchez-Riera F, Severson DK. In: Mobley DP, editor. Plastics from microbes. New York: Hanser; 1994. p. 93–137.
[2] Doi Y, Fukuda K, editors. Biodegradable plastics and polymers. Studies in polymer science vol. 12. Amsterdam: Elsevier; 1994.
[3] Coombes AGA, Meikle MC. Clin Mater 1994;17:35–67.
[4] Vert M, Schwarch G, Coudane J. J Macromol Sci, Pure Appl Chem 1995; A32:787–96.
[5] Hartmann MH. In: Kaplan DL, editor. Biopolymers from renewable resources. Berlin, Germany: Springer; 1998. p. 367–411.
[6] Ikada Y, Tsuji H. Macromol Rapid Commun 2000;21:117–32.
[7] Garlotta D. J Polym Environ 2001;9:63–84.
[8] Albertsson A-C, editor. Degradable aliphatic polyesters. Advances in polymer science, vol. 157. Berlin, Germany: Springer; 2002.
[9] Södergård A, Stolt M. Prog Polym Sci 2002;27:1123–63.
[10] Scott G. Biodegradable polymers. Principles and applications. 2nd ed. Dordrecht, The Netherlands: Kluwer Academic Publishers; 2002.
[11] Tsuji H. In: Doi Y, Steinbüchel A, editors. Biopolymers. Polyesters III, vol. 4. Weinheim, Germany: Wiley–VCH; 2002. p. 129–77.
[12] Auras R, Harte B, Selke S. Macromol Biosci 2004;4:835–64.
[13] Slager J, Domb AJ. Adv Drug Deliv Rev 2003;55:549–83.
[14] Tsuji H. Macromol Biosci 2005;5:569–97.
[15] Tsuji H, Ikada Y. Polymer 1999;40:6699–708.
[16] Tsuji H, Fukui I. Polymer 2003;44:2891–6.
[17] Tsuji H, Tezuka Y. Biomacromolecules 2004;5:1181–6.
[18] Brochu S, Prud'homme RE, Barakat I, Jérôme R. Macromolecules 1995; 28:5230–9.
[19] Schmidt SC, Hillmyer MA. J Polym Sci, Part B: Polym Phys 2001;39: 300–13.
[20] Yamane H, Sasai K. Polymer 2003;44:2569–75.
[21] Tsuji H, Ikada Y. Polymer 1995;36:2709–16.
[22] Tsuji H, Miyase T, Tezuka Y, Saha SK. Biomacromolecules 2005;6: 244–54.
[23] Tsuji H, Tezuka Y, Saha SK, Suzuki M, Itsuno S. Polymer 2005;46: 4917–27.
[24] Hoffman JD, Davis GT, Lauritzen Jr JI. In: Hannay NB, editor. Treatise on solid state chemistry. Crystalline and noncrystalline solids, vol. 3. New York: Plenum Press; 1976 [Chapter 7].
[25] Hoffman JD, Frolen LJ, Ross GS, Lauritzen Jr JI. J Res Natl Bur Stand A: Phys Chem 1975;79A:671–99.
[26] Vasanthakumari R, Pennings AJ. Polymer 1983;24:175–9.
[27] Abe H, Kikkawa Y, Inoue Y, Doi Y. Biomacromolecules 2001;2: 1007–14.
[28] Miyata T, Masuko T. Polymer 1998;39:5515–21.
[29] Huang J, Lisowski MS, Runt J, Hall ES, Kean RT, Buehler N, et al. Macromolecules 1998;31:2593–9.
[30] Baratian S, Hall ES, Lin JS, Xu R, Runt J. Macromolecules 2001;34: 4857–64.
[31] Di Lorenzo ML. Polymer 2001;42:9441–6.
[32] Iannace S, Nicolais L. J Appl Polym Sci 1996;64:911–9.
[33] Avrami M. J Chem Phys 1939;7:1103–12.
[34] Avrami M. J Chem Phys 1940;8:212–24.
[35] Avrami M. J Chem Phys 1941;9:177–85.
[36] Mandelkern L. Crystallization of polymers. New York: McGraw-Hill Book Company; 1964.
[37] Kolstad JJ. J Appl Polym Sci 1996;62:1079–91.
[38] Iannace S, Nicolasi L. J Appl Polym Sci 1997;64:911–9.
[39] Hoffman JD, Frolen LJ, Ross GS, Lauritzen Jr JI. J Res Natl Bur Stand A: Phys Chem 1975;79A:671–99.
[40] Hoffman JD, Davis GT, Lauritzen JI. In: Hannay NB, editor. Treatise on solid state chemistry: crystalline and non-crystalline solids. New York: Plenum; 1976. p. 497–614.
[41] Patel RM, Spruiell JE. Polym Eng Sci 1991;31:730–8.
[42] Migliaresi C, De Lollis A, Fambri L, Cohn D. Clin Mater 1991;8: 111–8.
[43] Ikada Y, Jamshidi K, Tsuji H, Hyon S-H. Macromolecules 1987;20: 904–6.